

LONGITUDINAL MOTION OF SINGLY CHARGED URANIUM IONS AT 9.5 GeV[†]

V. K. NEIL and H. L. BUCHANAN

Lawrence Livermore Laboratory, University of California, Livermore, California 94550, U.S.A.

and

R. K. COOPER

*Los Alamos Scientific Laboratory, University of California, Los Alamos,
New Mexico 87545, U.S.A.*

(Received July 11, 1978)

This work describes a computer code that can be used to study the non-relativistic motion of heavy ions in longitudinal phase space. We employ a distribution function and include the longitudinal electric self-field in an approximate fashion. We use the code to study the longitudinal compression of a pulse containing 50 μC of singly-charged uranium ions at 9.5 GeV. Results indicate that an initial pulse duration of 70 nsec can be reduced to 15 nsec in a distance of 600 m. The compression is achieved by applying a rather modest (~ 500 kV/m) time-varying longitudinal electric field over the first 500 m.

1. INTRODUCTION

Two requirements for heavy ion fusion (HIF) are very high current ($I \sim 10$ kA) and a pulse duration of about 10 nsec. Regardless of the method of accelerating ions to the energy required for HIF, the time duration of the pulse must be reduced and the current correspondingly increased between the accelerator and the target chamber. This compression possibly can be accomplished by applying a time-dependent axial electric field along the path to the chamber. This electric field is such as to decelerate particles in the front half of the pulse and accelerate particles in the back half of the pulse, but gives no net acceleration to the pulse.

If the required energy is obtained in an induction linear accelerator, some degree of compression can be achieved during acceleration by applying a time-varying electric field in addition to the accelerating electric field.

The purpose of this work is to investigate the longitudinal motion of particles in the pulse, taking

into account the longitudinal electric self-field of the particles in an approximate manner. Results of preliminary calculations demonstrate the feasibility of compressing the pulse carrying 5×10^{-5} coulombs of ^{238}U ions with charge state $q = 1$ at kinetic energy of 9.5 GeV. The energy in the beam is $\frac{1}{2}$ MJ. Two such beams from opposite directions deliver 1 MJ to the target. By applying physically realizable electric fields, the pulse duration is reduced from 70 nsec (FWHM) to about 15 nsec in a distance of 600 m.

2. EQUATIONS OF MOTION AND DISTRIBUTION FUNCTION

A computer code called INLIN describes the motion of particles in longitudinal phase space. The distance s along the beam path is taken as the independent variable. We define a reference particle that arrives at a position s at a time $T(s)$ given by

$$T(s) = \int_0^s \frac{ds'}{V(s')} \quad (1)$$

in which $V(s)$ is the speed of the reference particle at position s . Another particle in the beam has a different speed $v(s)$ and arrives at position s at a

[†] Work performed under the auspices of the U.S. Department of Energy by the Lawrence Livermore Laboratory and Los Alamos Scientific Laboratory under contract No. W-7405-Eng-48.

time $t \neq T(s)$. We choose the time difference τ given by

$$\tau(s) = t(s) - T(s) \quad (2)$$

as one dependent variable.

We employ non-relativistic dynamics; thus the reference particle has kinetic energy $K(s) = mV^2(s)/2$, with m the particle mass. This reference energy is independent of s if no net acceleration is imparted to the pulse. Other particles in the pulse have kinetic energy at position s given by $K(s) + w(s, t)$. Evidently

$$w = \frac{m}{2} \left[\left(\frac{ds}{dt} \right)^2 - V^2(s) \right]. \quad (3)$$

From Eq. (2) we have

$$\frac{d\tau}{ds} = \frac{dt}{ds} - \frac{1}{V(s)}. \quad (4)$$

Employing Eq. (3) to first order in w yields one first-order equation of motion,

$$\frac{d\tau}{ds} = -\frac{w}{mV^3}. \quad (5)$$

The longitudinal electric self-field E_s is treated in the simplest possible manner, in that we set

$$E_s = -\frac{g}{4\pi\epsilon_0} \frac{\partial\lambda}{\partial s} \quad (6)$$

in which λ is the charge per unit length in the pulse and g is a dimensionless quantity that depends on the cross-sectional dimensions of the beam and the surrounding walls. For a beam with radially uniform charge density out to radius $r = r_b$ and zero for $r > r_b$ inside a conducting pipe of radius $r = r_p$, the longitudinal electric self-field on axis is given by Eq. (6) with $g = 1 + 2 \ln(r_p/r_b)$. The field at $r = r_b$ is given by Eq. (6) with $g = 2 \ln(r_p/r_b)$. Particles in the beam are thought of as undergoing radial betatron oscillations and therefore sampling some average value of g . Equation (6) contains all the physics in the calculation. The rest is arithmetic. It is assumed (and insured in the calculations) that $\partial\lambda/\partial s = 0$ at the reference particle. With this consideration met, we have the reference particle,

$$\frac{dK}{ds} = qeE(s, 0) \quad (7)$$

in which $E(s, 0)$ is the electric field imparting the net acceleration to the pulse. If this electric field is uni-

form in s , the reference particle undergoes uniform acceleration "a" given by

$$a = \frac{qeE}{m}, \quad (8)$$

and we have

$$V^2(s) = V_0^2 + 2as, \quad (9)$$

in which V_0 is the speed of the reference particle at $s = 0$. The second equation of motion takes the form

$$\frac{dw}{ds} = qe[E(s, \tau) - E(s, 0)] - \frac{qeg}{4\pi\epsilon_0} \frac{\partial\lambda}{\partial s}. \quad (10)$$

We introduce a distribution $f(\tau, w, s)$ that describes the motion of particles in longitudinal $(\tau - w)$ phase area. At a given position s , the current $I(\tau, s)$ in the pulse is given by

$$I(\tau, s) = \int f(\tau, w, s) dw, \quad (11)$$

while the total charge Q in the pulse is given by

$$Q = \int I(\tau, s) d\tau, \quad (12)$$

and is independent of s .

In this formalism, we have knowledge of the distribution of particles in $\tau - w$ phase space at a given position s . We also calculate the current $I(\tau, s)$, but have no direct method of calculating $\lambda(\tau, s)$. However, for this calculation we can employ to a good approximation the relation

$$\frac{\partial\lambda}{\partial s} = -\frac{1}{V^2} \frac{\partial I}{\partial \tau}. \quad (13)$$

The uncertainty in the value of the quantity g in Eq. (6) outweighs the approximations inherent in Eq. (13).

The distribution function $f(\tau, w, s)$ obeys the equation

$$\frac{\partial f}{\partial s} + \frac{d\tau}{ds} \frac{\partial f}{\partial \tau} + \frac{dw}{ds} \frac{\partial f}{\partial w} = 0, \quad (14)$$

with $d\tau/ds$ and dw/ds given by Eqs. (5) and (10) respectively. The computational technique employed to solve Eq. (14) is described in the next section.

3. NUMERICAL METHOD AND INITIAL CONDITIONS

In the previous section we arrived at the following Eulerian representation of the Vlasov equation to be solved as an initial value problem:

$$\frac{\partial f}{\partial s} + A(w) \frac{\partial f}{\partial \tau} + B(\tau) \frac{\partial f}{\partial w} = 0. \quad (15)$$

Although we tried a number of explicit difference schemes, we found that in most of them, numerical diffusion significantly plagued the final outcome. As a result we have adopted a modification of the so-called method of splitting. The idea, due to Bargrinovskii and Godunov,¹ is to replace the complicated multi-dimensional operator of the first-order system

$$\begin{aligned} \frac{\partial u}{\partial t} &= Au, \\ A &= A_1 + A_2 + \dots + A_N, \end{aligned} \quad (16)$$

by successive application of the N one-dimensional operators A_n , thereby reducing the original multi-dimensional problem to a succession of one-dimensional problems. In the present case, the method is particularly straightforward because the coefficient in each of the advection terms [$A_1 = A(w)(\partial/\partial\tau)$, $A_2 = B(\tau)(\partial/\partial w)$] is independent of differential variables.

The strategy is then as follows: A grid of I columns and J rows is established in the variables τ and w with uniform intervals $\Delta\tau$ and Δw , so that $\tau_i = i\Delta\tau$ and $w_j = j\Delta w$. Furthermore, $s = n\Delta s$. The initial values of f_{ij}^0 at the grid points are selected as described below. To advance the calculations a step Δs , we first consider a particular column of the distribution. Using the values at the points in this column we can define a continuous function $g_i(w)$. Application of the operator $A_2 = B(\tau_i)\partial/\partial w$ amounts to a shift of the function $g_i(w)$ an amount $B(\tau_i)\Delta s$ in the $\pm w$ direction, keeping its shape unchanged. From this shifted function $g_i[w + B(\tau_i)\Delta s]$, new numbers are calculated and assigned to the appropriate grid points (j values) in the column. In practice, this is accomplished by fitting the points of a particular column to a continuous function using the method of cubic splines, shifting the function the proper increment, then picking off the desired values to refill the column. After all the columns ($i = 1, I$) have been treated in this manner, we have a new array of numbers in the grid which we designate as $f_{ij}^{1/2}$, the one-half

indicating the half of the operator A has been applied.

Application of the operator $A(w)\partial/\partial\tau$ is accomplished in an analogous manner, resulting in the array of numbers f_{ij}^1 . From this array the current $I(\tau)$ is calculated using Eq. (11), then a new operator $B(\tau)$ is obtained from Eqs. (10) and (13). If there is a net acceleration, Eq. (9) is used at each s step to calculate a new value of $V(s)$ to use in obtaining the new $B(\tau)$ as well as the new $A(w)$ from Eq. (5). The process is repeated each step until the desired solution is obtained.

If both A and B were functions of both τ and w , the general method would still apply but implementation would, of course, be more difficult. Stability of the solution is assured by satisfying the familiar Courant conditions, specifically

$$A(w) \frac{\Delta s}{\Delta \tau} \leq 1, \quad B(\tau) \frac{\Delta s}{\Delta w} \leq 1, \quad (17)$$

resulting in

$$\Delta s \leq \inf \left\{ \frac{\Delta \tau / A}{\Delta \tau / B} \right\}. \quad (18)$$

When Δs is in violation of these conditions, it is simply halved.

The area in $\tau - w$ phase space occupied by the particles is a constant of the motion. In our work we take this area to be determined by the requirements at the target chamber.² If the beam is to pass through an aperture of radius R in the chamber wall and be focussed in vacuum onto a target of radius r , chromatic aberration in the final focusing lens demands that the fractional momentum spread $\Delta p/p$ be less than r/R . For $r = 2$ mm and $R = 300$ mm, we have $\Delta p/p \sim 6 \times 10^{-3}$. The fractional energy spread is $w_{\max}/K = 2\Delta p/p \sim 10^{-2}$, so that $w_{\max} = 100$ MeV at $K = 10$ GeV. If the pulse duration at the target is of the order of 10 nsec, then the area in $\tau - w$ phase space is the order of 1 MeV- μ sec.

The initial distribution of particles is chosen as

$$f(\tau, w, 0) \propto \frac{\exp[-(w/DLW)^2]}{1 + \exp\{\eta[\tau/TT)^2 - 1]\}}, \quad (19)$$

with the normalization chosen from Eq. (12). The parameters DLW , η , and TT in Eq. (19) are chosen for each problem to be solved. The quantity η determines how sharply the distribution falls to zero along the τ axis, and TT is the half-width at half-maximum in τ .

4. FINAL COMPRESSION OF $\frac{1}{2}$ -MJ PULSE

We now consider the compression of a pulse containing $50 \mu\text{C}$ of singly charged ^{238}U with a mean kinetic energy $K = 9.5 \text{ GeV}$; two calculations are described. The value of the quantity g in Eq. (6) is somewhat optimistically chosen as 2. In Eq. (19) for the initial distribution $f(\tau, w, 0)$, we choose $\eta = 5$, $DLW = 20 \text{ MeV}$, $TT = 35 \text{ nsec}$, so that the area in $\tau - w$ phase space occupied by the particles is $\sim 1 \text{ MeV}\text{-}\mu\text{sec}$. This distribution is shown as the three-dimensional phase plot in Figure 1. The initial current $I(\tau, 0)$ is plotted vs τ in Figure 2, which also shows $I(\tau, s)$ at various values of s as the compression progresses.

The applied axial electric field is thought of as existing along the entire path length, and is therefore an average of the field that realistically would be supplied by discrete induction units. An advantage of the formalism employing s rather than t as the independent variable is that discrete units can be readily incorporated into the numerical solution when desired. At each position s the applied electric field is zero at $\tau = 0$ when the center of the bunch passes so that no net acceleration is present. The applied electric field used in the first calculation may be written in the form

$$E(s, \tau) = \dot{E}(s)\tau, \quad (20)$$

with $\dot{E}(s)$ given by

$$\dot{E}(s) = [8 + 22(s/500)](\text{kV/m})/\text{nsec}. \quad (21)$$

In Eq. (21) the distance s is in meters. At $s = 0$ and $\tau = -50 \text{ nsec}$ when the head of the pulse

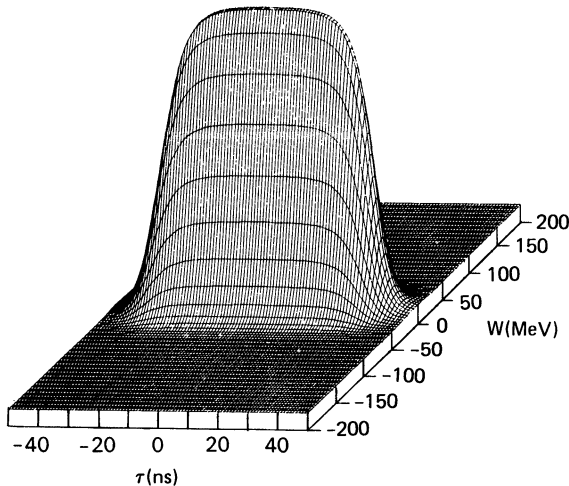


FIGURE 1 Initial distribution $f(\tau, w, 0)$.

arrives, $E(s, \tau) = -400 \text{ kV/m}$. At $\tau = +50 \text{ nsec}$ when the tail of the pulse arrives, $E(s, \tau) = +400 \text{ kV/m}$. As s increases and the compression occurs, $E(s, \tau)$ must change more rapidly in time, but need exist only during the time interval required for the beam to pass. For example, at $s = 400 \text{ m}$ we see from Figure 2 that the entire beam passes in 50 nsec . At this position, $E(s, \tau) = -640 \text{ kV/m}$ at $\tau = -25 \text{ nsec}$ and increases to $+640 \text{ kV/m}$ at $\tau = +25 \text{ nsec}$. At $s = 500 \text{ m}$, the entire beam passes in 30 nsec . At this position, $E(s, \tau) = -450 \text{ kV/m}$ at $\tau = -15 \text{ nsec}$ and increases to $+450 \text{ kV/m}$ at $\tau = +15 \text{ nsec}$.

The effectiveness of this compression method is apparent from Figure 2. After 500 m the full-width at half-maximum in τ has decreased to 16 nsec from an initial value of 70 nsec . Three-dimensional

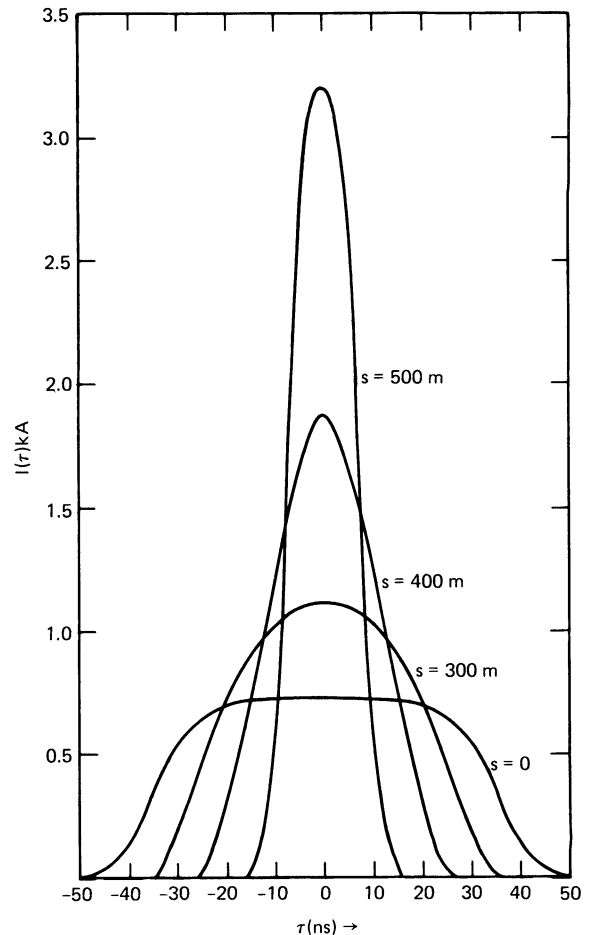


FIGURE 2 Current vs time at $s = 0, 300 \text{ m}, 400 \text{ m},$ and 500 m resulting from an applied electric field given by Eqs. (20) and (21).

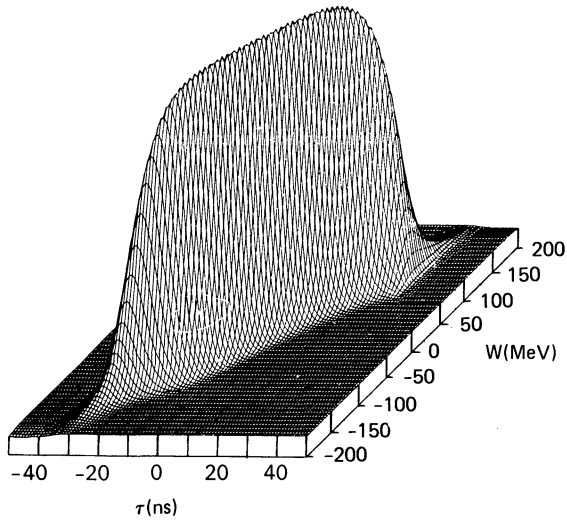


FIGURE 3 Distribution function $f(\tau, w, s)$ at $s = 300$ m resulting from an applied electric field given by Eqs. (20) and (21).

phase plots at $s = 300$ m and $s = 500$ m respectively are presented in Figures 3 and 4. Figure 4 shows that the distribution extends over the entire length of the grid in w , which extends from -200 MeV to $+200$ MeV. The full-width at half-maximum in w is about 200 MeV, so the energy spread after compression is somewhat larger than the desirable value of ~ 100 MeV discussed above.

During the calculation, about 2% of the initial distribution is lost off the grid in the w direction. This occurs because particles at the head and

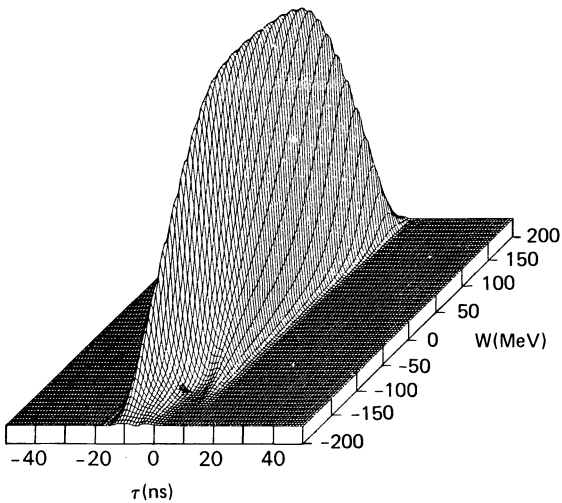


FIGURE 4 Distribution function $f(\tau, w, s)$ at $s = 500$ m resulting from an applied electric field given by Eqs. (20) and (21).

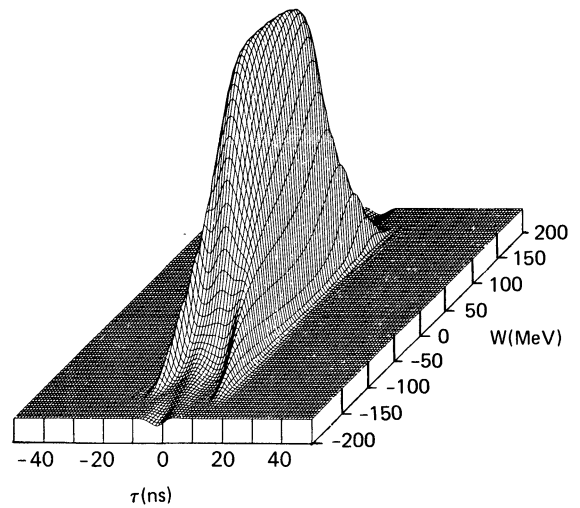


FIGURE 5 Distribution function $f(\tau, w, s)$ at $s = 600$ m resulting from an applied electric field given by Eqs. (20) and (22). The field is applied for the first 500 m only.

tail of the pulse are respectively decelerated and accelerated too quickly. Another calculation was performed using $\dot{E}(s)$ given by

$$\dot{E}(s) = [8 + 22(s/500)^2] \text{ kV/m-nsec.} \quad (22)$$

We found that the beam was not fully compressed at 500 m by this applied electric field. However, the beam was allowed to coast another 100 m with no applied electric field. The resulting $I(\tau)$ at 600 m is so similar to that in the previous calculation at

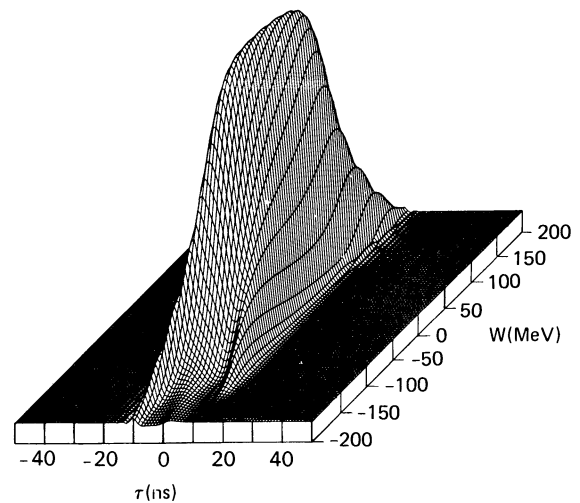


FIGURE 6 Distribution function $f(\tau, w, s)$ at $s = 600$ m resulting from an applied electric field given by Eqs. (20) and (22). The field is applied for 600 m.

500 m that it is not presented. The three-dimensional phase plot at 600 m is shown in Figure 5 for comparison with that in Figure 4 for the previous calculations. We see that the distribution is not so broad in w .

We performed a third calculation in which the compression field given by Eqs. (20) and (22) was applied over the entire 600 m. The resulting phase plot at 600 m is shown in Figure 6. Comparing Figures 5 and 6, we see that nothing is gained by applying the field over the additional 100 m. In the last 100 m the electric self-force is so strong that the applied field has little effect on particle motion.

Applying a compression field given by Eqs. (20) and (22) may also be advantageous in a practical sense, as it will probably cost less than applying a field given by Eqs. (20) and (21). This advantage may be outweighed by the cost of the additional 100 m of beam transport.

REFERENCES

1. K. A. Bargrinovskii and S. K. Godunov, *Dokl. Akad. Nauk. SSSR*, **15**, 431 (1957).
2. *ERDA Summer Study of Heavy Ions for Inertial Fusion*, Lawrence Berkeley Laboratory Report LBL-5543, December 1976, p. 13.